









Original Research

Role of Neuropeptide B/W Signaling in Modulating Intracellular Calcium in Human Skin Fibroblasts

Shashank Pandey^{1,*}, Elisa Peroni², Dagmar Jarkovska^{3,4},
Magdalena Chottova Dvorakova^{3,4}, Olivier Monasson², Michal Jirasko¹,
Tomas Chmelir^{3,4}, Radek Kučera¹

¹Department of Pharmacology and Toxicology, Faculty of Medicine in Pilsen, Charles University, 23200 Pilsen, Czech Republic

²Department of Chemistry, CY Cergy Paris Université, CNRS, BioCIS, 95000 Cergy Pontoise, France

³Department of Physiology, Faculty of Medicine in Pilsen, Charles University, 23200 Pilsen, Czech Republic

⁴Biomedical Center, Faculty of Medicine in Pilsen, Charles University, 23200 Pilsen, Czech Republic

*Correspondence: Shashank.Pandey@lfp.cuni.cz (Shashank Pandey)

Academic Editor: Thomas Heinbockel

Submitted: 27 September 2024 Revised: 30 November 2024 Accepted: 13 December 2024 Published: 20 February 2025

Abstract

Background: The neuropeptide B/W signalling system (NPB/W) has been identified in multiple body regions and is integral to several physiological processes, including the regulation of food intake and energy homeostasis. Recently, it has also been detected in human skin; however, its specific functions in this context remain to be thoroughly investigated. This study aims to identify the expression of neuropeptides B/W receptor 1 (NPBWR1) and neuropeptides B/W receptor 2 (NPBWR2) in human dermal fibroblasts of mesenchymal origin using genomic and proteomic techniques. We will also investigate the role of these receptors in cell proliferation and calcium signalling. **Methods:** The mRNAs for *NPBWR1* and *NPBWR2* were detected using quantitative PCR (qPCR) analysis and further validated by western blot and immunofluorescence analyses. Additionally, we synthesised ligands for these receptors, specifically hNPB (25–53) and hNPW (33–62), to investigate their effects on cell proliferation and intracellular calcium levels in human fibroblasts. **Results:** Our results demonstrated that hNPW (33–62) has anti-proliferative effect on human dermal fibroblasts and concentration of 0.1-μmol/L can significantly decrease intracellular calcium levels ($p < 0.05$). **Conclusion:** This finding suggests a potential role for the NPB/W signalling system in pathologies associated with impaired calcium handling, such as fibrosis. Furthermore, we observed that the proliferation of human fibroblasts was not affected by hNPB (25–53). Our findings could lead to the development of new therapeutic strategies for various skin conditions and improved wound healing.

Keywords: NPBWR1; NPBWR2; fibroblasts; calcium signalling; NPB; NPW

1. Introduction

G-protein-coupled receptors (GPCRs) represent a significant family of cell surface receptors and play a crucial role in detecting signals from the extracellular environment and regulating intercellular communication through various ligands. These receptors are integral to numerous physiological processes, such as inflammation and wound healing [1].

It is noteworthy that many GPCRs were characterised prior to the identification of their respective ligands. This holds true for the GPR7 and GPR8 receptors, which were initially described in the 1990s; their ligands were assigned a decade later [2]. The ligands associated with these receptors are two neuropeptides known as neuropeptide B (NPB) and neuropeptide W (NPW), which collectively form the NPB/W signalling system. In light of these ligands, the International Union of Basic and Clinical Pharmacology (IUPHAR) reclassified GPR7 and GPR8 as NPBWR1 and NPBWR2, respectively. It is also of interest to note that NPBWR2 is not expressed in rodent models [3].

The expression and function of the NPB/W signalling system have been investigated across various tissues and organs, including the central nervous system, endocrine glands, gastrointestinal tract, and adipocytes [2,4,5]. The findings from these studies indicate a range of functions associated with the NPB/W signalling system as a whole and its individual components.

At the organism level, the NPB/W signalling system is integral to the central regulation of food intake and the maintenance of energy homeostasis. At the cellular level, research has examined its effects on chondrocytes, smooth muscle cells, calvaria osteoblast-like cells, and preadipocytes, revealing diverse influences on cell proliferation and differentiation [4,6–8].

Neuropeptides are important signalling molecules synthesised and released by nerve cells and, in certain instances, non-neuronal cells. They are integral to a range of cellular responses, including within the skin. Depending on the presence of receptors specific to the released neuropeptides, different cell types serve as target cells within the skin. In human skin, mRNA expression has been identified



for all components of the NPB/W signalling system, including NPB, NPW, and their associated receptors [2]. However, determining the precise sources of NPB and NPW within the skin remains challenging when the analysis is conducted on a homogenised skin sample. Furthermore, identifying the target cells for these neuropeptides is complicated by the diverse array of cell types present in the skin: endothelial cells, keratinocytes, macrophages, lymphocytes, and fibroblasts.

Dermal fibroblasts are integral to the wound-healing process, facilitating both cell proliferation and the synthesis of extracellular matrix components [9]. As key cellular constituents of the skin, they play a significant role in maintaining homeostasis [10]. Research has identified several GPCRs on the fibroblast surface, enabling these cells to receive and respond to a variety of signals. The activation of GPCRs by specific stimuli can elicit a range of cellular responses, including alterations in gene expression, enhanced cell proliferation, and the secretion of extracellular matrix components. As a result, while fibroblast activation can promote effective wound healing and tissue repair, it may also lead to fibrosis due to excessive fibroblast production [10].

Furthermore, neuropeptide Y (NPY), a neuropeptide with functional similarities to NPB and NPW [2], has been shown to increase the proliferative capacity and migration of fibroblasts in both human and rat models. Additionally, NPY appears to delay the ageing of fibroblasts in these individuals [11,12]. However, the extent to which the NPB/W signalling system influences the behaviour of human fibroblasts remains to be fully elucidated.

This study's purpose was to investigate whether human skin fibroblasts express receptors associated with the NPB/W signalling system and examine the effects of NPB and NPW on these cells. The results may enhance our understanding of the potential role this signalling system plays in the physiological processes within the skin.

2. Materials and Methods

2.1 Cultivation of Primary Human Fibroblasts from Skin

Fibroblast cells were cultivated from human skin following a 4-mm punch biopsy, using a procedure similar to that developed by Vangipuram *et al.* in 2013 [13]. A 6-well plate was coated with gelatin (0.1%, G1393, Sigma-Aldrich, Saint Louis, MO, USA) at room temperature (RT) for 60 minutes. After this time, the gelatine solution was removed and replaced with 800 µL of Dulbecco's Modified Eagle Medium (DMEM), which contained high glucose, stable glutamine, and sodium pyruvate (Biowest, Nuaillé, France), supplemented with 20% foetal bovine serum (Sigma-Aldrich, Saint Louis, MO, USA) and 100 IU/mL of streptomycin/penicillin (A5955, Sigma-Aldrich, Saint Louis, MO, USA).

The skin biopsy was then dissected into evenly sized small pieces using a scalpel. Three to five pieces of skin

biopsy were placed in each well and incubated at 37 °C in a 5% CO₂ atmosphere. Daily monitoring of media evaporation was conducted, and 200 µL of DMEM was added every two days to compensate for evaporation during the first week. After one week, the volume of DMEM was increased to 2 mL. The medium was changed every 2–3 days until the fibroblasts reached confluence.

Once confluent, the plate was trypsinised, and the cells were transferred to two T75 flasks (passage 1). When the fibroblast cells became confluent in the T75 flasks, they were further transferred to three additional T75 flasks (passage 2). Finally, a 10% DMSO stock was prepared for the fibroblast cells at a concentration of 1×10^6 cells/mL per vial and stored at –80 °C. The cells were characterized by morphological features such as elongated, spindle-like cell bodies, round to oval cell nuclei. Additionally, we have also characterized the fibroblast cell lines by using anti-vimentin antibodies, a marker for fibroblast cell [14]. Additionally, we have also used antibiotic and antimycotic in the media to avoid the contamination, and cell lines were tested time to time for mycoplasma contamination. The data are available in **Supplementary materials**.

2.2 RNA Isolation and Reverse Transcription-quantitative Polymerase Chain Reaction (RT-qPCR) Analysis

RNA was isolated from fibroblast cells utilising RNeasy Micro Kits (Qiagen, Hilden, Germany), following the manufacturer's instructions. To eliminate any contaminating DNA, 1 unit of DNase per microgram of total RNA (Invitrogen, Carlsbad, CA, USA) was incorporated into the procedure. The isolated RNA was reverse-transcribed using Superscript III Reverse Transcriptase (Invitrogen, Carlsbad, CA, USA) for 50 minutes at 42 °C. Two micrograms of total RNA were utilised to synthesise single-stranded cDNA. The qPCR analysis was conducted as previously outlined [15].

The primers were specifically designed to amplify target sequences corresponding to the following nucleotides: vimentin (forward: AAGACACTATTGGC-CGCCTG (1507–1526), reverse: ATTCACGAAGGT-GACGAGCC (1559–1578)), *NPBWR1* (forward: TGAC-CTCGAGCCTTCTTGGA (3674–3693), reverse: CGTAT-GAAGGGCAACGACCT (3860–3879)), and *NPBWR2* (forward: GCCAACGTCTCTCAGGACAA (360–379), reverse: TCACCGTCTTCATCTTGGGC (512–531)).

The qPCR was performed on an iCycler (Bio-Rad, Prague, Czech Republic). The final volume of each assay was 15 µL. Each reaction contained 3.5 µL of diluted cDNA, 7.5 µL of iQ SYBR Green Supermix (Bio-Rad, Prague, Czech Republic), 0.15 µL of each primer (at a concentration of 20 nmol/L), and 3.7 µL of ultrapure water. All qPCR analyses were executed in duplicate following a strict protocol: an initial denaturation step at 95 °C for 10 minutes, succeeded by 45 cycles of amplification (95 °C for 20

seconds, 60 °C for 20 seconds, and 72 °C for 20 seconds). A melting curve was subsequently generated by heating the samples from 65 °C to 95 °C, during which fluorescence was continuously monitored to confirm the specificity of each amplicon. Each pair of primers yielded a single peak in the melting curve and exhibited a single band of the expected size upon agarose gel electrophoresis.

Data quantification was performed using Optical System Software (Bio-Rad, Prague, Czech Republic), and normalisation of *NPBWR1* and *NPBWR2* was achieved using vimentin.

2.3 Extraction of Protein and WB Analysis

Fibroblast cells were cultured in a T75 flask until they reached confluence. Upon achieving confluence, the cells were treated with trypsin, and the resulting suspension was centrifuged to separate the pellet. The pellet was then washed twice with phosphate-buffered saline (PBS) and solubilised in lysis buffer prior to homogenisation. The lysate was centrifuged at 10,000 ×g for 10 minutes at 4 °C to eliminate debris and the supernatant was collected. The total protein concentration was determined using Bradford dye (Bio-Rad, Hercules, CA, USA).

A total of 25 µg of protein was loaded onto a 10% SDS-PAGE gel under reducing conditions (2% v/v β-mercaptoethanol). The gel was transferred to a nitrocellulose membrane (0.2 µm; Bio-Rad, Hercules, CA, USA) at a constant current of 220 mA at RT for 2 hours. To prevent non-specific binding, the membrane was blocked with a 5% milk powder solution in PBS-Tween (PBS pH 7.4 with 0.1% TWEEN 20) for 1 hour.

After blocking, the membrane was incubated overnight at 4 °C with either anti-NPBWR1 (1:500; bs-8618R, Bioss Antibodies Inc, Woburn, MA, USA) or anti-NPBWR2 (1:100; BP2-86659, Novus Biologicals, Centennial, CO, USA). Alternatively, it was incubated with anti-β-actin (1:250; bs0061R, Bioss Antibodies Inc, Woburn, MA, USA) for 1 hour at RT.

The membrane underwent three washes (10 minutes each) with PBS-Tween (0.1%). The blot was treated with horseradish peroxidase (HRP)-conjugated anti-IgGs (1:4000, A16116, Thermo Fisher Scientific, Frederick, MD, USA) for 45 minutes at RT. The membrane was washed three additional times with PBS-Tween (0.1%). The resulting blots were developed using the Clarity™ Western ECL kit (Bio-Rad, Hercules, CA, USA). Imaging was conducted using the ChemiDoc MP system (Bio-Rad, Hercules, CA, USA), and the data were analysed with Image Lab software (Bio-Rad, Hercules, CA, USA).

2.4 Immunofluorescence Analysis

A glass slide was placed inside a sterile petri dish and 50 µL of a 1 × 10⁶ cells/mL dilution was added to the glass slide. The slide was incubated overnight at 37 °C with 5% CO₂. After incubation, the cells adhered to the glass slide.

The cells were then washed with PBS at RT and fixed with ice-cold acetone for 10 minutes at RT.

For permeabilisation, the cells were treated with 0.3% Triton X-100 in PBS for 5 minutes at RT. The cells were washed three times with PBS and blocked with 5% normal goat serum in PBS at RT for 1 hour. The cells were then incubated overnight at 4 °C with anti-NPBWR1 (1:200; bs-8618R, Bioss Antibodies Inc., Woburn, MA, USA), anti-NPBWR2 (1:150; BP2-86659, Novus Biologicals, Centennial, CO, USA), or anti-vimentin (1:100; Cell Signaling Technology, Danvers, MA, USA).

Afterwards, the samples were washed three times with PBS and incubated for 1 hour at RT with FITC-conjugated anti-rabbit IgGs (1:300; F9887, Sigma, St. Louis, MO, USA). Finally, the cells were submerged in DAPI mounting medium (Sigma, St. Louis, MO, USA). Images were captured at 10× magnification using a fluorescence microscope (Olympus IX83) and analysed using ImageJ 1.53a, (Wayne Rasband, NIH, Bethesda, MD, USA).

2.5 Peptide Synthesis and Purification

All Fmoc-protected amino acids, Fmoc-Wang resins, N,N'-Diisopropylcarbodiimide (DIC), Ethyl (hydroxyimino)cyanoacetate (Oxyma), and 2-(1H-Benzotriazole-1-yl)-1,1,3,3-tetramethylaminium tetrafluoroborate (TBTU) were purchased from Iris Biotech GmbH (Marktredwitz, Germany). Peptide-grade DMF was obtained from Biosolve (Dieuze, France). Triisopropylsilane (TIS), DIPEA, and diethyl ether (Et₂O) were purchased from Sigma Aldrich (Milan, Italy).

Peptides hNPB (25–53) and hNPW (33–62) were synthesised in solid-phase using a microwave-assisted protocol (MW-SPPS) on a Liberty Blue™ automated peptide synthesiser (CEM Corporation, Matthews, NC, USA), following the Fmoc/tBu strategy. The syntheses were performed on preloaded Wang TG resins: Fmoc-Ala-WANG TG and Fmoc-Trp(Boc)-WANG TG (0.25 mmol/g).

Fmoc-deprotections were conducted using a solution of 20% (v/v) piperidine in DMF. Peptide assembly was carried out by repeating the standard MW-SPPS coupling cycle for each amino acid, utilising Fmoc-protected amino acids (5 equivalents, 0.2 M in DMF), OxymaPure® (5 equivalents, 1 M in DMF), and DIC (5 equivalents, 0.5 M in DMF).

2.6 Deprotection, Cleavage, Purification and Characterization of Peptide

Cleavage from the resin and side-chain deprotection was achieved by treatment with a TFA/TIS/water solution (95: 2.5: 2.5 v/v/v, 1 mL/100 mg of resin-bound peptide). The cleavage was carried out for approximately four hours with vigorous shaking at RT. Each resin was filtered off, and the solution was concentrated by flushing with N₂. Each peptide was precipitated from cold Et₂O, centrifuged, and lyophilized.

Table 1. Peptide sequence and analytical data of hNPB (25–53) and hNPW (33–62).

Peptide	Sequence	Retention Time (min)	Mass Calculated [M+3H] ³⁺	Mass Found [M+3H] ³⁺	HPLC Purity
hNPB (25–53)	WYKPAAGHSSYSVGRAAGLLSGLRRSPYA	1.58	1027.50	1027.47	98%
hNPW (33–62)	WYKHVASPRYHTVGRAAGLLMGLRRSPYLW	1.69	1182.07	1182.42	98%

Peptides were synthesized in solid-phase using a microwave-assisted protocol on a Liberty Blue™ automated peptide synthesizer following the Fmoc/tBu strategy. Synthetic peptides were purified by RP-HPLC and analyzed by LC-MS analysis. The peptides were obtained with more than 95% purity. The solvent systems used were 0.1% TFA in H₂O (A) and 0.1% TFA in CH₃CN (B), and the gradient was 10%–90% B in 3 min. hNPB, human neuropeptide B; hNPW, human neuropeptide W.

Lyophilized crude peptides were purified by a semi-preparative Waters reverse-phase high-performance liquid chromatography (RP-HPLC) (Waters Corporation, Milford, MA, USA) on a Phenomenex Jupiter C18 (10 µm, 250 mm × 10 mm) column (Phenomenex, Castel Maggiore, Italy) at 4 mL/min. The solvent systems used were 0.1% TFA in H₂O (A) and 0.1% TFA in CH₃CN (B) (as shown in Table 1). All peptides obtained exhibited a purity greater than 95%.

Characterisation of the peptides was performed using analytical reverse-phase ultra-performance liquid chromatography coupled with electrospray ionisation mass spectrometry (RP-UPLC ESI-MS). The measurement was performed using a Waters Acquity UPLC connected to a Waters 3100 ESI-SQD mass spectrometer, utilising a Luna Omega PS C18 column (1.6 µm, 2.1 × 50 mm) maintained at 35 °C and operated at a flow rate of 0.5 mL/min. The solvent systems used were Solvent System A (0.1% TFA in H₂O) and Solvent System B (0.1% TFA in CH₃CN). Data acquisition and processing were conducted using MassLynx software from Waters (Milford, MA, USA).

2.7 Cell Proliferation Assay

50 µL of 1×10^5 cells were seeded per well onto a flat-bottom 96-well cell culture plate. Following this, 25 µL of peptide solution was added to each well. The peptide concentrations used were 0.004 µmol/L, 0.04 µmol/L, 0.4 µmol/L, and 4 µmol/L, prepared in DMEM media containing 10% FBS and 0.1% streptomycin/penicillin. An additional 25 µL of DMEM media with 10% FBS and 0.1% streptomycin/penicillin was added to each well.

This resulted in a total volume of 100 µL per well, corresponding to final peptide concentrations of 0.001 µmol/L, 0.01 µmol/L, 0.1 µmol/L, and 1 µmol/L, respectively. The cells were then incubated at 37 °C with 5% CO₂ for 48 hours.

After 48 hours, 10 µL of the cell proliferation reagent WST-1 (Roche Diagnostics GmbH, Germany) was added to each well, and the plate was incubated again at 37 °C with 5% CO₂ for four hours. The absorbance was measured at a wavelength of 450 nm using a microplate reader (Synergy H1, Agilent BioTek, Santa Clara, CA, USA).

2.8 Measurement of Intracellular Calcium

A 12-well or 9-well plate was utilised for this experiment. 500 µL of a solution containing 1×10^6 cells/mL was added to each well. The cells were initially suspended in glutamine-free DMEM media supplemented with 10% FBS and 0.1% streptomycin/penicillin. They were then incubated overnight at 37 °C in an environment with 5% CO₂.

Following incubation, the media were removed, and the cells were washed with Ca²⁺-free Tyrode solution. After washing, the cells were treated with 5 µmol/L Fura-2-AM for 30 minutes at 37 °C. The Fura-2-AM solution (F1221, Thermo Fisher Scientific Life Technology, Eugene, OR, USA) was then removed, and the cells were washed with 1 mL of Tyrode solution for 10 minutes at 37 °C. After the final wash, the cells were exposed to 1 mL of 0.1 µmol/L hNPW (33–62) or 0.1 µmol/L hNPB (25–53) in Ca²⁺-free Tyrode solution.

The intracellular calcium levels in the cells were measured using the IonOptix HyperSwitch Myocyte Calcium and Contractility System (IonOptix LLC, Westwood, CA, USA). The Tyrode solution had the following composition (in mmol/L): NaCl 137, KCl 4.5, MgCl₂ 1, CaCl₂ 2, Glucose 10, HEPES 5, with the pH adjusted to 7.4 using NaOH. All chemicals were obtained from Sigma-Aldrich (St. Louis, MO, USA). Offline analysis was conducted using IonWizard 6.5 software (IonOptix LLC, Westwood, CA, USA).

2.9 Statistical Analysis

Data were presented using a box and whisker plot. Moreover, univariate analysis was done by the non-parametric Mann–Whitney U- test for 2 groups by Kruskal–Wallis test for more groups, while multivariate analysis was done using three way ANOVA models where also an experiment number effect nested in cell line effect was included. Dunnett's adjustment for a multiple comparison with one control group was used in the ANOVA models. Statistical analyses were conducted with GraphPad Prism 7.02 (GraphPad Software, Boston, MA, USA) or SAS 9.4M8 (TS1M8) (producer SAS Institute Inc., Cary, NC, USA). Statistical significance was set as $p < 0.05$.

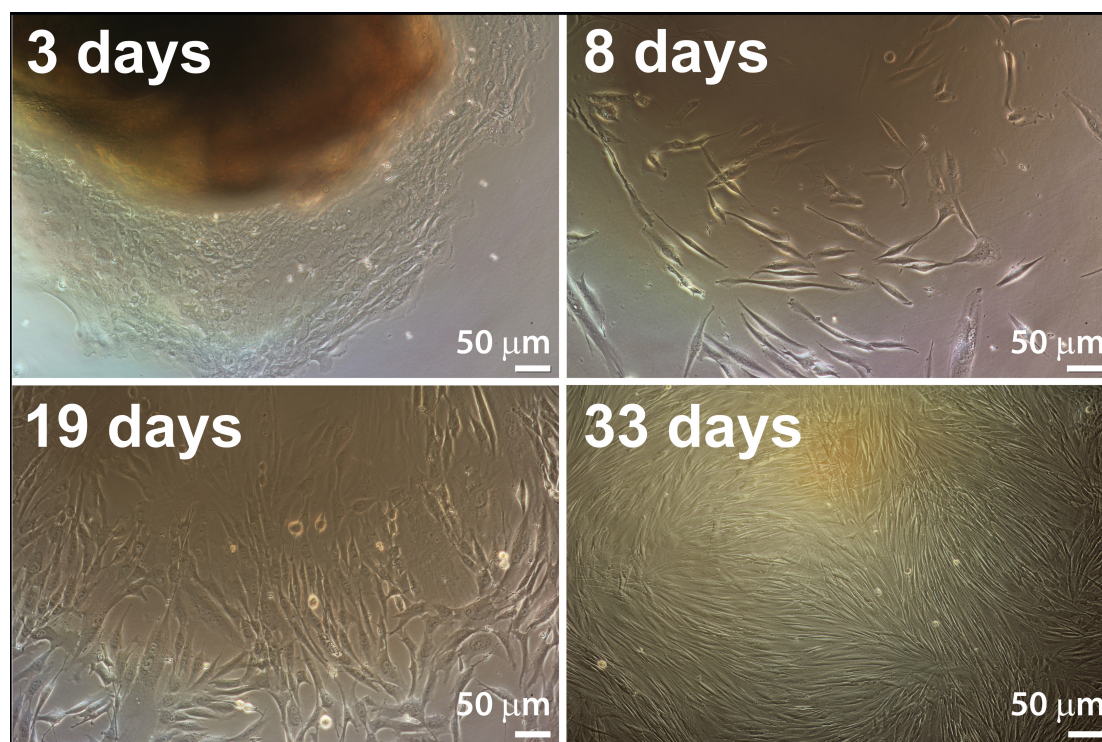


Fig. 1. Dermal fibroblasts from human skin. Cultivation of dermal fibroblasts was done from skin biopsies. The growth of keratinocytes was observed within 3 days and full confluency of fibroblast was achieved in 33 days (scale bar 50 µm).

3. Results

3.1 Cultivation of Fibroblasts from Human Skin

Skin fibroblasts were successfully developed from dissected human skin biopsies. We observed that keratinocytes migrated out of the biopsy tissue within the first week. The outgrowth of keratinocytes was followed by the growth of fibroblast cells within 7 to 10 days. DMEM high-glucose media supplemented with 20% FBS promoted the growth of fibroblasts over keratinocytes. Consequently, the keratinocytes were depleted after two passages. Finally, the fibroblast cells were fully developed in 30 to 40 days, as confirmed by their morphology (shown in Fig. 1). A 10% DMSO stock was prepared, and we designated these stocks as PASSAGE-0 for use in our experiments. All experiments were conducted with cell lines that had not been passaged more than four times after PASSAGE-0 to avoid any mutations [16]. Similar cell lines were also used to prepare hiPSC and astrocytes [17].

10% DMSO stock were prepared. We considered these stocks as PASSAGE-0 and used them for our experiments. All the experiments were done with the cell lines which were not passaged more than 4 times after PASSAGE-0 to avoid any mutations.

3.2 Identification of *NPBWR1*/*NPBWR2*

RT-qPCR analysis was conducted across nine different cell lines. The presence of mRNA for vimentin was confirmed in all samples, validating the accuracy of all preced-

ing steps. The Cq value of vimentin was used to compare the expression levels of *NPBWR1* and *NPBWR2* in each sample. mRNA for *NPBWR2* was detected in all samples, whereas mRNA for *NPBWR1* was present in only 6 out of the 9 samples. Notably, the relative expression of mRNA for *NPBWR2* was approximately 32 times higher than that of mRNA for *NPBWR1* (as shown in Fig. 2).

These findings were further confirmed using proteomic approaches, including Western blotting (WB) and immunofluorescence analysis. Commercially available antibodies against vimentin, *NPBWR1*, and *NPBWR2* were employed to detect both receptors in fibroblast cells. Our results indicated that all anti-vimentin-positive cells were also immunoreactive for both anti-*NPBWR1* and anti-*NPBWR2* antibodies, suggesting the presence of these receptors on the surface of all fibroblasts of mesenchymal origin.

Western blot analysis was performed on ten different cell lines. We observed a single immunogenic band for *NPBWR1* at approximately 50 kDa in all ten samples (as shown in Fig. 3a). The expression level of *NPBWR1* was about 0.3 times lower compared to β -actin (as shown in Fig. 3c). However, we did not detect any band corresponding to the *NPBWR2* receptor at 50 kDa. This may be due to the antibodies being unable to recognise the denatured form of *NPBWR2* or because the concentration of *NPBWR2* in fibroblast cells was too low for detection via WB analysis (as shown in Fig. 3b). Interestingly, immunofluorescence

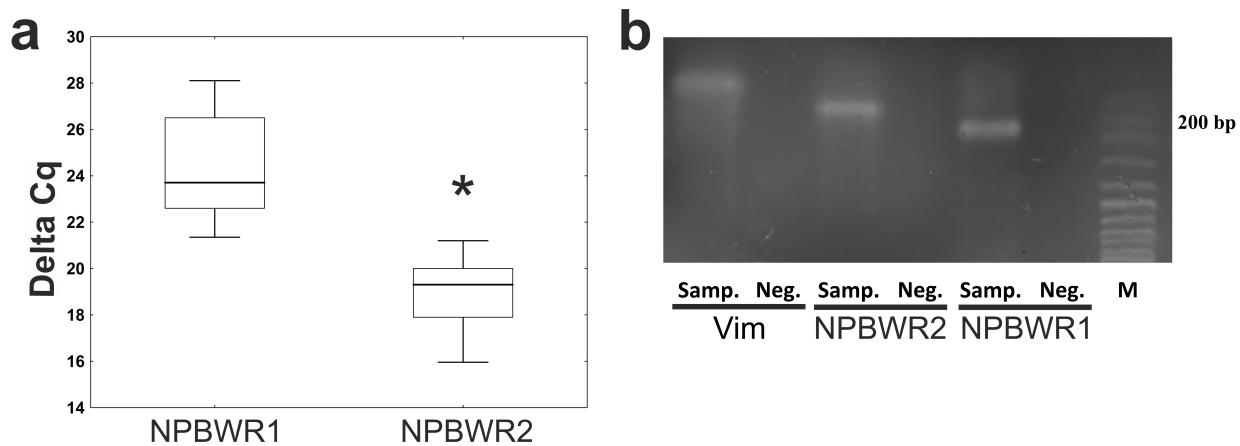


Fig. 2. Detection of mRNAs of neuropeptides B/W receptor (*NPBWR1*/*NPBWR2*) by RT-qPCR analysis. Different fibroblast cell lines were used for detection of mRNAs. We have observed the presence of *NPBWR1* in 6 out of 9 samples and *NPBWR2* in all the samples. (a) Data are presented as ΔCq values (compared to vimentin) to indicate differences in expression between *NPBWR1* and *NPBWR2*, represented by “*”. Relative expression of mRNA for *NPBWR2* was about 32 times higher than expression of mRNA for *NPBWR1*. (b) Agarose gel electrophoresis of qPCR products of *NPBWR1* and *NPBWR2* amplified. Samp, sample; Vim, vimentin; Neg, water (negative control); M, marker.

analysis successfully detected NPBWR2 in 5 out of 5 samples, indicating that the anti-NPBWR2 antibody was able to recognise only the conformational form of NPBWR2 (as shown in Fig. 4).

These results were further validated by proteomic approach through WB and immunofluorescence analysis.

3.3 Role of *NPBWR1*/*NPBWR2* in Ca^{2+} Signaling and Cell Proliferation

We have synthesised the ligands of NPBWR1/NPBWR2, specifically hNPB (25–53) and hNPW (33–62), as detailed in Table 1. These synthetic peptides were utilised to investigate the influence of NPBWR1/2 signalling on cell proliferation and intracellular calcium levels. The viability of the treated cells was assessed using the WST-1 assay, and all experiments were conducted across 11 different experiments with 5 cell lines for NPB and 17 different experiments with 11 cell lines for NPW.

Cells were treated with four distinct concentrations of hNPB (25–53) and hNPW (33–62): 0.001 mol/L, 0.01 mol/L, 0.1 mol/L, and 1 mol/L. Overall, as illustrated in Fig. 5, we did not observe any statistically significant effects of hNPB (25–53) ($p = 0.7338$ Kruskal-Wallis test, $p = 0.4180$ ANOVA), while hNPW (33–62) shows a negative proliferative effect ($p = 0.0464$ Kruskal-Wallis test, $p = 0.0248$ ANOVA) on cell viability as analyzed by multivariate in three-way ANOVA analysis (Fig. 5) and also by univariate Kruskal-Wallis test. Post hoc power analysis of hNPW (33–62) shows the power of testing as 50.8% with used sample size per groups ($n = 17$) to detect observed difference of 3.5 as statistically significant.

Additionally, we conducted an experiment to estimate the intracellular concentration of Ca^{2+} in fibroblasts after treating the cells with 0.1 $\mu\text{mol/L}$ of either hNPB (25–53) or hNPW (33–62). This part of the study involved 7 different experiments with 5 different cell lines and we used a concentration of 0.1 $\mu\text{mol/L}$ for the peptides. Our findings showed that hNPW (33–62) effectively interfered with intracellular calcium signalling, resulting in a decrease in the intracellular Ca^{2+} level in fibroblasts ($p = 0.0248$ Mann-Whitney U-test, $p = 0.0109$ ANOVA for hNPW (33–62) effect).

Conversely, we did not find any significant impact of hNPB (25–53) ($p = 0.1517$ Mann-Whitney U-test, $p = 0.1618$ ANOVA for hNPB (25–53) effect) on intracellular Ca^{2+} concentration, as depicted in Fig. 6. The results were analysed by measuring dual fluorescence intensity at excitation wave lengths of 340 nm and 380 nm.

4. Discussion

Fibroblasts are a diverse group of cells responsible for producing extracellular matrix. They exhibit transcriptional and functional differences depending on their tissue origin as well as variations within the same tissue [18]. Fibroblasts derived from mesenchymal tissues express the filamentous protein vimentin, while those of epithelial origin express fibroblast-specific protein and fibroblast activation protein [10]. Fibroblasts represent the predominant type of stromal cells in the skin, working with epithelial cells and skin-resident immune cells to constitute the cutaneous structure. These cells serve as vital components of the skin framework, primarily through the production of collagen [19]. However, the role of skin fibroblasts extends beyond structural support; they are integral to various physiolog-

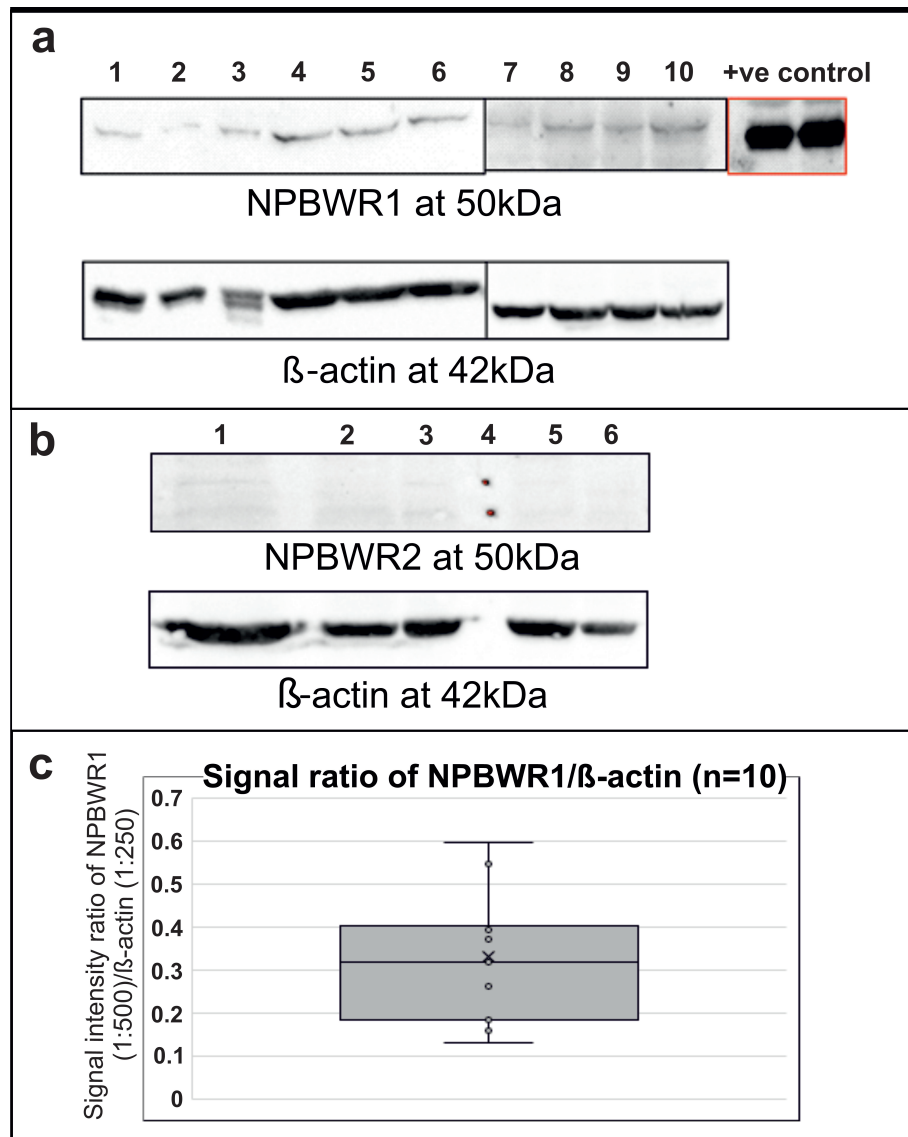


Fig. 3. Identification of NPBWR1/NPBWR2 by western blotting (WB) analysis. Different fibroblast cell lines were used to identify NPBWR1/NPBWR2. (a,c) We have observed the immunogenic band of NPBWR1 in 10 out of 10 samples (lane 1 to 10) at 50 kDa, but the expression of NPBWR1 was ~0.3 times lower than β -actin. Rat heart lysate was used as a positive control. (b) We didn't observe any band of NPBWR2 receptor at 50 kDa, the data of five cell lines were shown. Uncropped pictures were attached to **Supplementary materials**.

ical and pathological processes, including wound repair, healing, and the modulation of malignant and immune responses within the skin [19].

The functions of fibroblasts are largely mediated through the release of diverse substances in response to specific environmental signals. Fibroblasts detect these signals via their membrane-bound GPCRs [18], which are critical for numerous physiological functions. To date, over 800 GPCRs have been identified in the human genome. Many GPCRs are found in the cell membrane of fibroblasts, with fibroblasts in different organs containing different combinations of receptors [10].

The objective of this study was to investigate the expression of NPBWR1 and NPBWR2 in human dermal fibroblasts of mesenchymal origin, which were cultivated from human skin biopsies, utilising both genomic and proteomic methodologies. A range of approaches were implemented to accomplish this objective.

Immunocytochemical experiments confirmed that all fibroblasts analysed were of mesenchymal origin, as evidenced by specific immunoreactivity with the anti-vimentin antibody. Furthermore, these experiments established the presence of both receptors, NPBWR1 and NPBWR2, in all fibroblast samples.

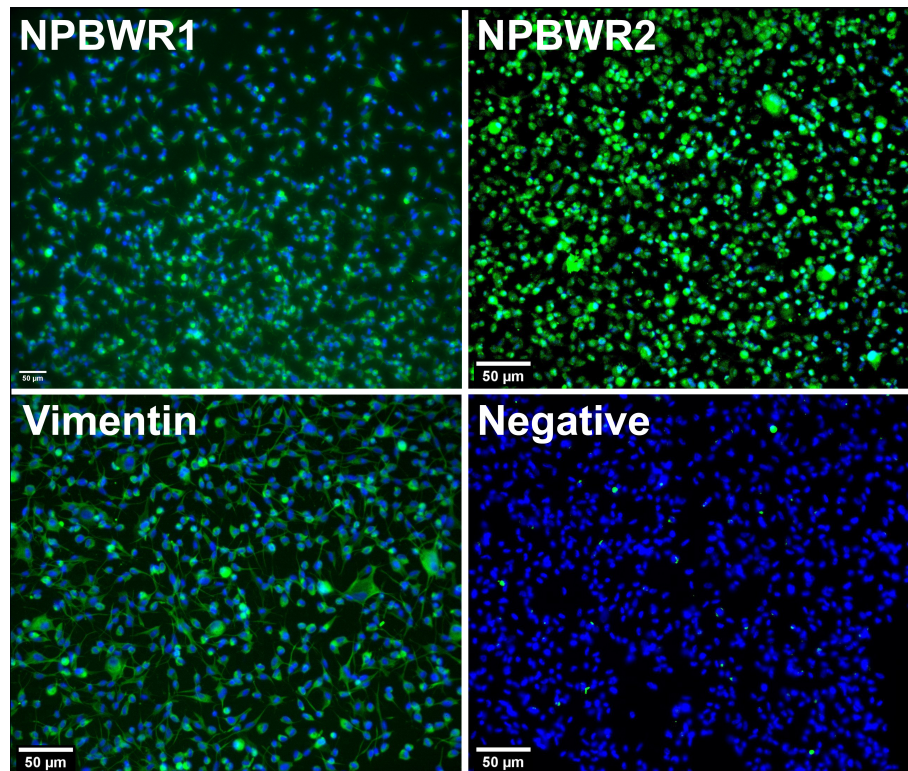


Fig. 4. Identification of NPBWR1/NPBWR2 by immunofluorescence analysis. Different fibroblast cell lines were used for identification of NPBWR1 ($n = 6$) and NPBWR2 ($n = 5$). The cells were incubated with anti-NPBWR1, anti-NPBWR2, vimentin (positive control), and without primary antibodies (negative control). Fluorescein isothiocyanate (FITC)-conjugated anti-rabbit IgGs (green channel) were used to detect the primary antibodies along with 4',6-diamidino-2-phenylindole (DAPI) (blue channel) for nuclear staining (scale bar 50 μm). Images were taken using fluorescence microscope.

Analysis of the genomic data indicated significant quantitative differences in the expression levels of the two receptors. Notably, the mRNA for the *NPBWR2* receptor was expressed at levels several times higher than that of the *NPBWR1* receptor. The relatively low expression of the *NPBWR1* gene may explain the undetectable mRNA levels in some samples, as it is reasonable to assume that the gene copy number in these cases fell below the detection threshold of the employed analysis method.

However, at the protein level, we successfully demonstrated the presence of the NPBWR1 receptor in all tested cell lines. These findings are consistent with those reported by Philippeos *et al.* [20], who detected very low-level expression of genes for *NPB*, *NPBWR1* and *NPBWR2* in some samples of papillary or reticular human skin dermis.

The NPB/W signalling system has been implicated in a variety of important physiological processes. It plays a role in modulating pain transmission, regulating behavioural responses to stress, managing inflammatory neuropathies, and controlling feeding behaviours. Additionally, this system influences the activity of endocrine glands, regulates vascular smooth muscle tone, and contributes to the metabolism of adipocytes. These effects are primarily mediated through the receptors NPBWR1 and NPBWR2

[2]. Subcutaneous adipocytes, similar to the fibroblasts we examined, are derived from mesenchymal cells and express both *NPBWR1* and *NPBWR2*. Prior research has explored the impact of the NPB/W signalling system on the proliferation and differentiation of various cell types. Notably, a study has indicated that NPB influences the proliferation of preadipocytes and facilitates their differentiation into mature adipocytes in porcine models [4]. Additionally, NPB exerts a proliferative effect on brown primary preadipocytes in rats, promoting the differentiation of white preadipocytes into adipocytes [4,21].

Thus, the NPB/W signalling system exhibits a positive proliferative effect on cultured pig and rat adipocytes, a phenomenon that is mediated by NPBWR1 receptor [4,21]. Conversely, both NPB and NPW have been identified as inhibitors of the proliferative activity in cultured rat calvarial osteoblast-like cells despite these cells also expressing NPBWR1 [8].

Intriguingly, NPB does not affect the proliferation of rat insulin-producing cells [5]. Similarly, our findings indicate that NPB does not influence the proliferation of human fibroblasts, while NPW shows a negative proliferative effect. Notably, skin fibroblasts display a significantly higher expression of NPBWR2 than NPBWR1, which may

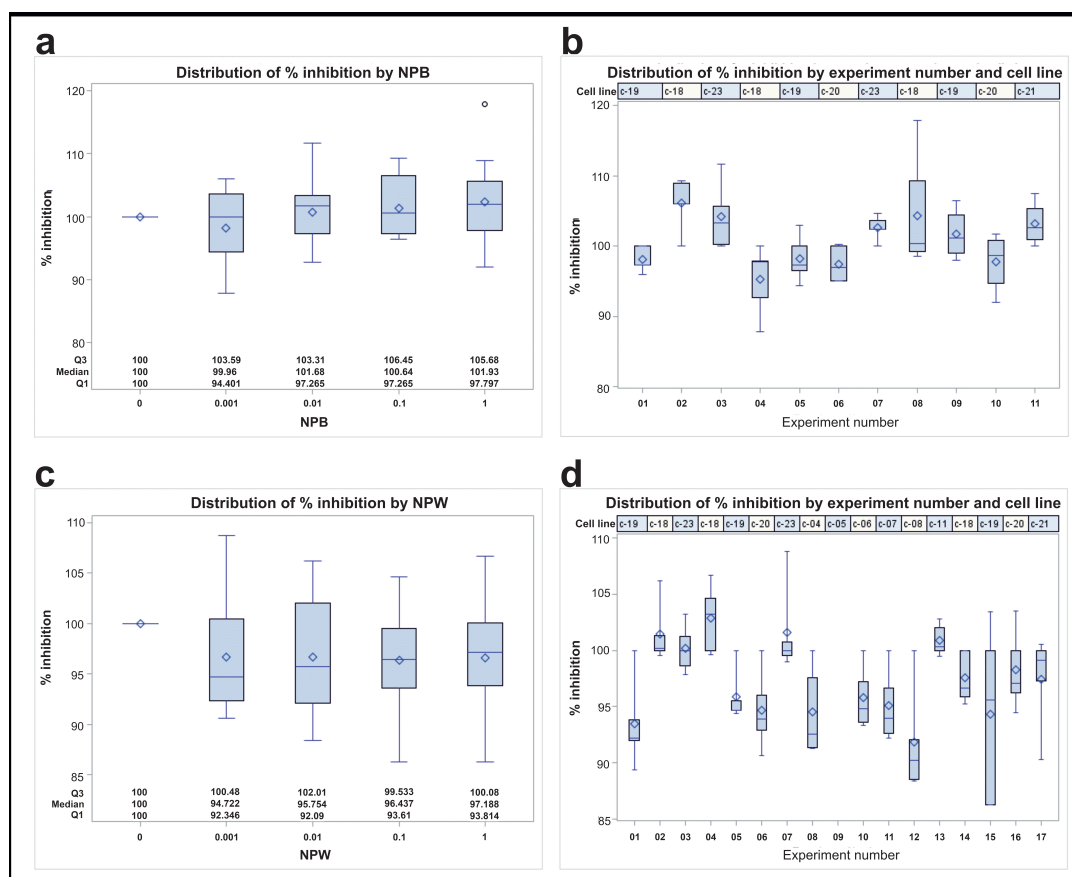


Fig. 5. Impact of hNPB (25–53) and hNPW (33–62) on cell proliferation. The cells were treated with different concentrations of peptide solution 0.001- $\mu\text{mol/L}$, 0.01- $\mu\text{mol/L}$, 0.1- $\mu\text{mol/L}$, 1- $\mu\text{mol/L}$ in DMEM media with 10% FBS and 0.1% streptomycin/penicillin. (a,c) For NPB and NPW respectively. Distribution of % inhibition was analyzed. (b,d) NPB and NPW respectively. We did not observe any statistically significant impact of hNPB (25–53), while hNPW (33–62) shows a negative proliferative effect on human dermal fibroblast ($p = 0.0464$ Kruskal-Wallis test, $p = 0.0248$ ANOVA). The data was analyzed by multivariate three-way ANOVA analysis and univariate Kruskal-Wallis test.

account for the observed differences in the effects of the signalling system on fibroblast and adipocyte proliferation.

These varying results across different cell types suggest that the mere presence of NPBWR1 is insufficient to mediate the positive proliferative effects of neuropeptides B and W. It is plausible that an additional cofactor, yet to be identified, is involved in the regulation of this process.

In fibroblasts, calcium signalling plays an essential role in various cellular processes, including proliferation, migration, extracellular matrix formation, and myofibroblast differentiation [22]. Our study demonstrated that intracellular calcium levels were significantly influenced by NPW, while NPB did not elicit a similar effect. This finding corresponds with our observation of a markedly higher expression of *NPBWR2* compared to *NPBWR1*, as *NPBWR2* exhibits a greater affinity for NPW [23], whereas *NPBWR1* has an increased affinity for NPB [24].

Notably, we found that NPW leads to a decrease in intracellular calcium levels, which contrasts with its reported effects in vascular smooth muscle cells [6] and ventricu-

lar cardiomyocytes [25]. It is important to note that both studies mentioned above conducted in muscle cell types and utilised rat cells that exclusively express *NPBWR1* [2]. This implicates calcium voltage-gated channels as active participants in those contexts. Consequently, we speculate that the effect of NPW on fibroblasts, which inherently lack calcium voltage-gated channels, may be mediated through an alternative pathway.

The function of NPW in regulating intracellular calcium levels could bear resemblance to neuropeptide Y (NPY), which exhibits differential actions based on the receptor involved. Specifically, NPY interaction with receptor Y1 results in enhanced calcium transients [26], whereas interaction with receptor Y2 leads to diminished calcium levels [27]. Future investigations should explore the potential interaction between *NPBWR1* and *NPBWR2*, given that cross-talk among NPY receptors has been previously documented [28], suggesting a similar phenomenon may occur with NPW receptors.

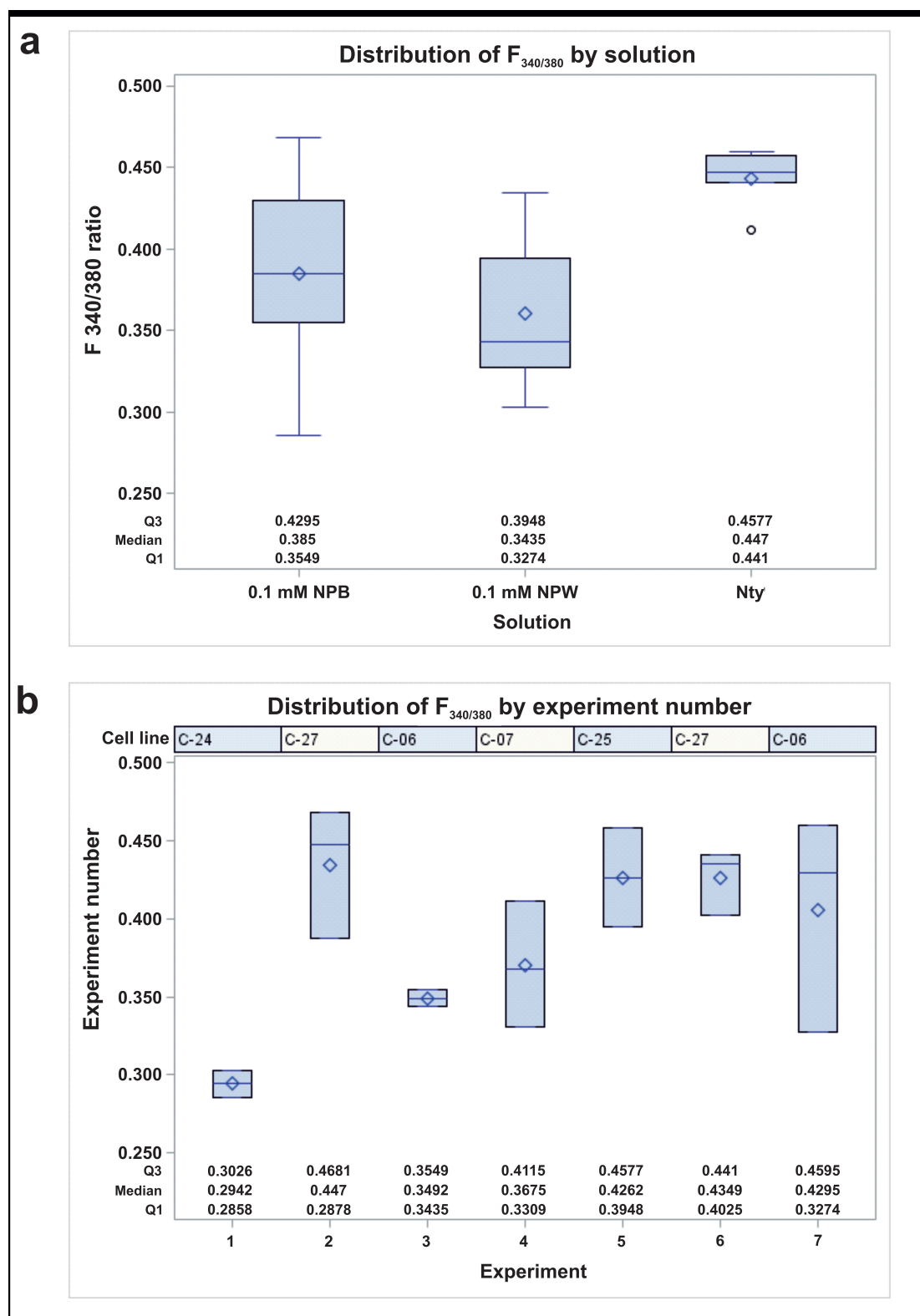


Fig. 6. Impact of hNPB (25–53) and hNPW (33–62) on intracellular Ca^{2+} . The cells were treated with peptide solution consist of 0.1- μ mol/L-hNPW (33–62) or 0.1- μ mol/L-hNPB (25–53) in Ca^{2+} free Tyrode solution. We have observed that hNPW (33–62) was able to inhibit the intracellular Ca^{2+} of the fibroblast. The difference was statistically significant ($p = 0.0248$ Mann–Whitney U-test, $p = 0.0109$ ANOVA for hNPW (33–62)) when compared to cells without peptide treatment. However, we did not observe any significant impact of hNPB (25–53) ($p = 0.1517$ Mann–Whitney U-test, $p = 0.1618$ ANOVA). (a) Distribution of $F_{340/380}$ by experiment number. (b) NTy represents “ Ca^{2+} free Tyrode solution without peptides”.

Moreover, past research indicates that NPBWR2 is coupled with Gi/o proteins [29]. Therefore, we conclude that the NPW-mediated effect on calcium levels in human skin fibroblasts is likely facilitated through the inhibition of adenylate cyclase, resulting in decreased cAMP levels and subsequent reduction in PKA activity. This decreased PKA activity contributes to diminished activation of various calcium channels and reduced phosphorylation of IP3 receptors [30], collectively leading to an overall decrease in intracellular calcium levels.

This finding may explain the observed decrease in intracellular calcium levels after the application of NPW. The lower concentration of intracellular calcium suggests that NPW might act as an intracellular calcium chelator. This is supported by the significant reduction in fibroblast intracellular calcium levels when treated with 0.1 $\mu\text{mol/L}$ of hNPW (33–62). The NPB/W signalling system may become activated under certain pathological conditions, such as fibrosis, where calcium signalling plays a significant role in the disease's pathophysiology [31]. Research has shown that fibroblasts from patients with cystic fibrosis or cancer exhibit an increase in intracellular calcium concentration, highlighting the importance of calcium regulation in these cells. Moreover, intracellular calcium is essential for the migration of fibroblasts [32]. Variations in intracellular Ca^{2+} levels furthermore play a crucial role in determining whether cells commit to remaining in the premitotic interphase or transitioning into mitosis. Additionally, these variations can influence cell-to-cell adhesion by remodelling cortical actin and facilitating the recruitment of cadherins and beta-catenin into intercellular junctions [22]. Notably, it has also been observed that increased intracellular Ca^{2+} can facilitate wound healing [23,24].

The wound healing process consists of three phases: haemostasis/inflammation, proliferation, and remodelling [33]. Calcium levels play a key role in the healing process, particularly during its initial phases [34]. However, during the final remodelling phase, elevated intracellular calcium may contribute to the excessive formation of scar tissue. A study conducted by Ishise *et al.* [35] in 2015 found that increased intracellular calcium levels in fibroblasts activate the nuclear factor kappa-light-chain-enhancer of activated B (NF- κ B) pathway, which subsequently enhances fibronectin production. This mechanism may be responsible for hypertrophic scar contracture. Furthermore, the study revealed that fibroblasts in hypertrophic scars exhibit significantly higher calcium levels compared to those in normal skin [36]. These findings indicate that NPW could potentially prevent the development of hypertrophic scars by reducing intracellular calcium levels. Additionally, intracellular calcium chelators, such as basic fibroblast growth factor (bFGF), can be used to prevent apoptosis in cells by effectively regulating intracellular Ca^{2+} concentrations [37,38].

The precise sources of natural mediators for the receptors NPB and NPW within the skin remain to be fully elucidated. Current evidence confirms the presence of these mediators in the bloodstream, with NPB also identified in the skin dermis and subcutaneous adipose tissue [4,20,39]. Additionally, sensory nerve fibres may represent another potential source of these receptors, as NPB has been detected in neuron bodies within the dorsal root ganglia (DRG) [15], NPW, on the other hand, has not. These findings suggest that NPB and NPW may exert both endocrine and paracrine effects on skin fibroblasts.

5. Conclusion

In summary, we have successfully demonstrated the expression of the receptors NPBWR1 and NPBWR2 in human mesenchymal fibroblasts through both genomic and proteomic methodologies. However, it is noteworthy that the expression levels for NPBWR1 and NPBWR2 were insufficient for detection via WB analysis. Furthermore, our research indicates that this signalling system is involved in the regulation of intracellular calcium levels; specifically, hNPW (33–62) appears to modulate intracellular calcium signalling and decrease the concentration of Ca^{2+} within fibroblasts. Additional experiments will be necessary to comprehensively understand the mechanisms at play, especially in *in vivo* contexts.

Limitation of the Study

In this study, we were not able to detect NPBWR2 in human dermal fibroblast through western blot, while similar antibodies were able to detect NPBWR2 in immunofluorescence analysis. This may relate to antibody specificity or receptor denaturation during western blot. To overcome this problem, one can use different methodology such as complete gel blot or mass spectrometry analysis for further validation of the results.

Availability of Data and Materials

The datasets used and/or analyzed during the current study are available from the corresponding author on reasonable request.

Author Contributions

SP, MCD designed the research study. SP, MCD, DJ, EP, OM, TC, MJ performed the research. RK provided help and advice. SP, DJ, EP, OM, TC, MJ analyzed the data. MCD, SP wrote the manuscript. All authors have participated sufficiently in the work and agreed to be accountable for all aspects of the work. All authors contributed to editorial changes in the manuscript. All authors read and approved the final manuscript.

Ethics Approval and Consent to Participate

The study was conducted according to the guidelines of the Declaration of Helsinki, and approved by the Ethical Committee, University Hospital Pilsen and Faculty of Medicine in Pilsen, Charles University, Edvarda Beneše 1128/13, 30599 Pilsen – Czech Republic (email: etick-akomise@fnplzen.cz) on 19th June 2019. WRITTEN INFORMED consent was obtained from any adults participating in this study.

Acknowledgment

I would like to express my sincere gratitude to the reviewers for their valuable and constructive comments, which have significantly enhanced the quality of this work. I also wish to acknowledge Natalie Bergman (professional english translator, Pilsen, Czech Republic) and Dr. Nancy Linder (professional english translator, Laboratoire BIO-CIS, BETIC/Peptlab, CY Cergy Paris Université, France) for their support in reviewing the English language. Special thanks to Ladislav Pecen (Statistician, Department of Pharmacology and Toxicology, Faculty of Medicine in Pilsen, Charles University, Czech Republic) for his support in analyzing the data.

Funding

This research was supported by the Cooperation Program, research area Medical Diagnostics and Basic Medical Sciences.

Conflict of Interest

The authors declare no conflict of interest.

Supplementary Material

Supplementary material associated with this article can be found, in the online version, at <https://doi.org/10.31083/FBL26760>.

References

- [1] Rahman MM, Islam MR, Mim SA, Sultana N, Chellappan DK, Dua K, *et al.* Insights into the Promising Prospect of G Protein and GPCR-Mediated Signaling in Neuropathophysiology and Its Therapeutic Regulation. *Oxidative Medicine and Cellular Longevity*. 2022; 2022: 8425640. <https://doi.org/10.1155/2022/8425640>.
- [2] Chottova Dvorakova M. Distribution and Function of Neuropeptides W/B Signaling System. *Frontiers in Physiology*. 2018; 9: 981. <https://doi.org/10.3389/fphys.2018.00981>.
- [3] Sakurai T. NPBWR1 and NPBWR2: Implications in Energy Homeostasis, Pain, and Emotion. *Frontiers in Endocrinology*. 2013; 4: 23. <https://doi.org/10.3389/fendo.2013.00023>.
- [4] Wojciechowicz T, Kolodziejski PA, Billert M, Strowski MZ, Nowak KW, Skrzypski M. The Effects of Neuropeptide B on Proliferation and Differentiation of Porcine White Preadipocytes into Mature Adipocytes. *International Journal of Molecular Sciences*. 2023; 24: 6096. <https://doi.org/10.3390/ijms24076096>.
- [5] Billert M, Sassek M, Wojciechowicz T, Jasaszili M, Strowski MZ, Nowak KW, *et al.* Neuropeptide B stimulates insulin secretion and expression but not proliferation in rat insulin producing INS 1E cells. *Molecular Medicine Reports*. 2019; 20: 2030–2038. <https://doi.org/10.3892/mmr.2019.10415>.
- [6] Ji L, Zhu H, Chen H, Fan W, Chen J, Chen J, *et al.* Modulation of CaV1.2 calcium channel by neuropeptide W regulates vascular myogenic tone via G protein-coupled receptor 7. *Journal of Hypertension*. 2015; 33: 2431–2442. <https://doi.org/10.1097/HJH.0000000000000723>.
- [7] Wang R, Zheng C, Jiang W, Xie X, Liao R, Zhou G. Neuropeptide W regulates proliferation and differentiation of ATDC5: Possible involvement of GPR7 activation, PKA and PKC-dependent signalling cascades. *Journal of Cellular and Molecular Medicine*. 2019; 23: 2093–2102. <https://doi.org/10.1111/jcmm.14118>.
- [8] Ziolkowska A, Rucinski M, Tyczewska M, Malendowicz LK. Neuropeptide B (NPB) and neuropeptide W (NPW) system in cultured rat calvarial osteoblast-like (ROB) cells: NPW and NPB inhibit proliferative activity of ROB cells. *International Journal of Molecular Medicine*. 2009; 24: 781–787. <https://doi.org/10.3892/ijmm.00000292>.
- [9] Thangapazham RL, Darling TN, Meyerle J. Alteration of skin properties with autologous dermal fibroblasts. *International Journal of Molecular Sciences*. 2014; 15: 8407–8427. <https://doi.org/10.3390/ijms15058407>.
- [10] Dwivedi NV, Datta S, El-Kersh K, Sadikot RT, Ganti AK, Batra SK, *et al.* GPCRs and fibroblast heterogeneity in fibroblast-associated diseases. *FASEB Journal: Official Publication of the Federation of American Societies for Experimental Biology*. 2023; 37: e23101. <https://doi.org/10.1096/fj.202301091>.
- [11] Aveleira CA, Ferreira-Marques M, Cortes L, Valero J, Pereira D, Pereira de Almeida L, *et al.* Neuropeptide Y Enhances Progerin Clearance and Ameliorates the Senescent Phenotype of Human Hutchinson-Gilford Progeria Syndrome Cells. *The Journals of Gerontology. Series A, Biological Sciences and Medical Sciences*. 2020; 75: 1073–1078. <https://doi.org/10.1093/geron/g12280>.
- [12] Thangaratnarajah C, Dinger K, Vohlen C, Klaudt C, Nawabi J, Lopez Garcia E, *et al.* Novel role of NPY in neuroimmune interaction and lung growth after intrauterine growth restriction. *American Journal of Physiology. Lung Cellular and Molecular Physiology*. 2017; 313: L491–L506. <https://doi.org/10.1152/ajplung.00432.2016>.
- [13] Vangipuram M, Ting D, Kim S, Diaz R, Schüle B. Skin punch biopsy explant culture for derivation of primary human fibroblasts. *Journal of Visualized Experiments: JoVE*. 2013; e3779. <https://doi.org/10.3791/3779>.
- [14] Ostrowska-Podhorodecka Z, Ding I, Norouzi M, McCulloch CA. Impact of Vimentin on Regulation of Cell Signaling and Matrix Remodeling. *Frontiers in Cell and Developmental Biology*. 2022; 10: 869069. <https://doi.org/10.3389/fcell.2022.869069>.
- [15] Pandey S, Tuma Z, Peroni E, Monasson O, Papini AM, Chottova Dvorakova M. Identification of NPB, NPW and Their Receptor in the Rat Heart. *International Journal of Molecular Sciences*. 2020; 21: 7827. <https://doi.org/10.3390/ijms21217827>.
- [16] Neumann E, Riepl B, Knedla A, Lefèvre S, Tarner IH, Grifka J, *et al.* Cell culture and passaging alters gene expression pattern and proliferation rate in rheumatoid arthritis synovial fibroblasts. *Arthritis Research & Therapy*. 2010; 12: R83. <https://doi.org/10.1186/ar3010>.
- [17] Juráková V, Széky B, Zapletalová M, Fehér A, Zana M, Pandey S, *et al.* Assessment and Evaluation of Contemporary Approaches for Astrocyte Differentiation from hiPSCs: A Modeling Paradigm for Alzheimer's Disease. *Biological Procedures Online*. 2024; 26: 30. <https://doi.org/10.1186/s12575-024-00257-y>.

- [18] Plikus MV, Wang X, Sinha S, Forte E, Thompson SM, Herzog EL, *et al.* Fibroblasts: Origins, definitions, and functions in health and disease. *Cell*. 2021; 184: 3852–3872. <https://doi.org/10.1016/j.cell.2021.06.024>.
- [19] Wang L, Wang B, Kou E, Du L, Zhu Y. New insight into the role of fibroblasts in the epithelial immune microenvironment in the single-cell era. *Frontiers in Immunology*. 2023; 14: 1259515. <https://doi.org/10.3389/fimmu.2023.1259515>.
- [20] Philippeos C, Telerman SB, Oulès B, Pisco AO, Shaw TJ, Elgueta R, *et al.* Spatial and Single-Cell Transcriptional Profiling Identifies Functionally Distinct Human Dermal Fibroblast Subpopulations. *The Journal of Investigative Dermatology*. 2018; 138: 811–825. <https://doi.org/10.1016/j.jid.2018.01.016>.
- [21] Wojciechowicz T, Billert M, Dhandapani P, Szczepankiewicz D, Wasielewski O, Strowski MZ, *et al.* Neuropeptide B promotes proliferation and differentiation of rat brown primary preadipocytes. *FEBS Open Bio*. 2021; 11: 1153–1164. <https://doi.org/10.1002/2211-5463.13128>.
- [22] Berridge M, Lipp P, Bootman M. Calcium signalling. *Current Biology*. 1999; 9: R157–R159. [https://doi.org/10.1016/S0960-9822\(99\)80101-8](https://doi.org/10.1016/S0960-9822(99)80101-8).
- [23] Tanaka H, Yoshida T, Miyamoto N, Motoike T, Kurosu H, Shibata K, *et al.* Characterization of a family of endogenous neuropeptide ligands for the G protein-coupled receptors GPR7 and GPR8. *Proceedings of the National Academy of Sciences of the United States of America*. 2003; 100: 6251–6256. <https://doi.org/10.1073/pnas.0837789100>.
- [24] Brezillon S, Lannoy V, Franssen JD, Le Poul E, Dupriez V, Lucchetti J, *et al.* Identification of natural ligands for the orphan G protein-coupled receptors GPR7 and GPR8. *The Journal of Biological Chemistry*. 2003; 278: 776–783. <https://doi.org/10.1074/jbc.M206396200>.
- [25] Pandey S, Jarkovska D, Tuma Z, Smrhova T, Chottova Dvorakova M. Regulation of Prepro-Neuropeptide W/B and Its Receptor in the Heart of ZDF Rats: An Animal Model of Type II DM. *International Journal of Molecular Sciences*. 2022; 23: 15219. <https://doi.org/10.3390/ijms232315219>.
- [26] Heredia MDP, Delgado C, Pereira L, Perrier R, Richard S, Vassort G, *et al.* Neuropeptide Y rapidly enhances [Ca²⁺]_i transients and Ca²⁺ sparks in adult rat ventricular myocytes through Y1 receptor and PLC activation. *Journal of Molecular and Cellular Cardiology*. 2005; 38: 205–212. <https://doi.org/10.1016/j.yjmc.2004.11.001>.
- [27] Lewis CJ, Evans RJ, Neild TO. Inhibition of vasoconstriction and Ca²⁺ currents mediated by neuropeptide Y Y2 receptors. *Journal of Smooth Muscle Research*. 1999; 35: 147–156. <https://doi.org/10.1540/jsmr.35.147>.
- [28] Silva AP, Carvalho AP, Carvalho CM, Malva JO. Functional interaction between neuropeptide Y receptors and modulation of calcium channels in the rat hippocampus. *Neuropharmacology*. 2003; 44: 282–292. [https://doi.org/10.1016/S0028-3908\(02\)00382-9](https://doi.org/10.1016/S0028-3908(02)00382-9).
- [29] Scanes CG. Opening a New Door: Neuropeptide W (NPW) Is a Novel Inhibitory Secretagogue for GH and Prolactin Acting via the Gi Protein-Coupled NPBWR2. *Endocrinology*. 2016; 157: 3394–3397. <https://doi.org/10.1210/en.2016-1518>.
- [30] Janssen LJ, Mukherjee S, Ask K. Calcium Homeostasis and Ionic Mechanisms in Pulmonary Fibroblasts. *American Journal of Respiratory Cell and Molecular Biology*. 2015; 53: 135–148. <https://doi.org/10.1165/ajrcmb.2014-0269TR>.
- [31] Gnegy ME, Erickson RP, Markovac J. Increased calmodulin in cultured skin fibroblasts from patients with cystic fibrosis. *Biochemical Medicine*. 1981; 26: 294–298. [https://doi.org/10.1016/0006-2944\(81\)90004-1](https://doi.org/10.1016/0006-2944(81)90004-1).
- [32] Wei C, Wang X, Zheng M, Cheng H. Calcium gradients underlying cell migration. *Current Opinion in Cell Biology*. 2012; 24: 254–261. <https://doi.org/10.1016/j.ceb.2011.12.002>.
- [33] Xing L, Chen B, Qin Y, Li X, Zhou S, Yuan K, *et al.* The role of neuropeptides in cutaneous wound healing: a focus on mechanisms and neuropeptide-derived treatments. *Frontiers in Bioengineering and Biotechnology*. 2024; 12: 1494865. <https://doi.org/10.3389/fbioe.2024.1494865>.
- [34] Subramaniam T, Fauzi MB, Lokanathan Y, Law JX. The Role of Calcium in Wound Healing. *International Journal of Molecular Sciences*. 2021; 22: 6486. <https://doi.org/10.3390/ijms22126486>.
- [35] Ishise H, Larson B, Hirata Y, Fujiwara T, Nishimoto S, Kubo T, *et al.* Hypertrophic scar contracture is mediated by the TRPC3 mechanical force transducer via NFκB activation. *Scientific Reports*. 2015; 5: 11620. <https://doi.org/10.1038/srep11620>.
- [36] Wang W, Qian Y, Cui L. Determination of intracellular calcium ions in fibroblasts of contracted scar. *Zhongguo Xiu Fu Chong Jian Wai Ke Za Zhi = Chinese Journal of Reparative and Reconstructive Surgery*. 1998; 12: 329–331. (In Chinese)
- [37] Magnelli L, Cinelli M, Turchetti A, Chiarugi VP. Bcl-2 overexpression abolishes early calcium waving preceding apoptosis in NIH-3T3 murine fibroblasts. *Biochemical and Biophysical Research Communications*. 1994; 204: 84–90. <https://doi.org/10.1006/bbrc.1994.2429>.
- [38] Lynch K, Fernandez G, Pappalardo A, Peluso JJ. Basic fibroblast growth factor inhibits apoptosis of spontaneously immortalized granulosa cells by regulating intracellular free calcium levels through a protein kinase Cdelta-dependent pathway. *Endocrinology*. 2000; 141: 4209–4217. <https://doi.org/10.1210/en.do.141.11.7742>.
- [39] Grzelak T, Wedrychowicz A, Grupinska J, Pelczynska M, Sperling M, Mikulska AA, *et al.* Neuropeptide B and neuropeptide W as new serum predictors of nutritional status and of clinical outcomes in pediatric patients with type 1 diabetes mellitus treated with the use of pens or insulin pumps. *Archives of Medical Science: AMS*. 2019; 15: 619–631. <https://doi.org/10.5114/aoms.2018.75818>.